ACADEMIA ROMÂNĂ
Revue Roumaine de Chimie
http://web.icf.ro/rrch/

Rev. Roum. Chim.,
2021, *66*(5), 391–397
DOI: 10.33224/rrch.2021.66.5.01

SYNTHESIS AND CHARACTERIZATION OF ZINC OXIDE BASED POLY VINYLALCOHOL NANOCOMPOSITE MEMBRANES AND THEIR FUEL CELL MEASUREMENT

Mallikarnunagouda PATIL*

P.G. Department of Chemistry, Basaveshwar Science College, Bagalkot-587101, Karnataka, INDIA

Received May 22, 2020

Nanocomposite membranes of poly(vinyl alcohol) (PVA) and Zinc oxide (ZnO) were prepared and while preparing the membrane the varying concentration of Zinc oxide nanoparticles were added *i.e.* 2.5, 5, and 10 wt. % gravimetrically. All prepared nanocomposite membranes were crosslinked using glutaraldehyde. The prepared membranes were assessed for FTIR. A scanning electron microscopy tool was used to study the surface morphology of the prepared membranes. SEM results show that the ZnO fillers were distributed uniformly across the membrane matrix. The synthesized membranes were assessed for fuel cell analysis. An increasing amount of ZnO elevated ion exchange capacity and consequently proton conductivity of the membranes. The addition of the small amount of ZnO as a filler enhanced membrane performance in terms of proton conductivity properties. Membranes presented good proton conductivity (in the range of 10^{-2} S cm^{-1}) and lesser H_2.

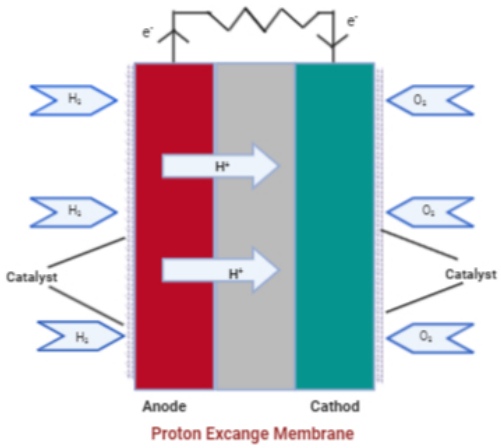

INTRODUCTION

In recent years, global energy shortage and ecological pollution problems have created opportunities for fuel cells to replace the existing technologies in a variety of applications. Some common areas of application of fuel cells embody power for stationary, portable and transport applications. They are used to provide electricity and heat in large stationary applications.[1–3] They are also used to provide power in areas that are difficult to serve by the national grid. In sectors such as telecom, they find use in providing backup power. Another promising space of application is their use in transportable devices like mobile phones. Due to their light weight and higher operating times, they are seen as a good alternative to solid batteries. Their application in transport finds its roots in their ability to satisfy the rigorous emission norms. As far as the world fuel cell industry is concerned, most of the activities are concentrated in regions of North America, Europe, Japan and Korea. The areas of experience vary from R&D to element manufacture and system integration. Fundamental and applied R&D is carried out in universities as well as by commercial players. A large variety of companies are concerned in element producing and system integration. The governments in these regions offer robust funding for the event of the electric cell sector. India's electric cell business isn't quite developed as compared to the on top of mentioned regions. Even

* Corresponding author: mallupatil04@gmail.com

then, it can be considered a very important and emerging market. An economy growing at a fast pace and a country in need of energy to sustain the growth are the factors that strengthen India's position as a prospective market for fuel cells. New national energy policies of the country that promote the growth of hydrogen and fuel cell technologies add to the market potential of fuel cells in India.[4–7]

This high growth rate essentially signifies upliftment of large number of population from poverty to India's growing middle class. This growing middle class is causing a consumer boom in Indian market which is contributing to India's growth.[8–10]

Energy Landscape

India is the world's sixth largest energy consumer, accounting for almost 3.4% of the global energy consumption. Due to continuous high growth rates seen over the last few years, the demand for energy has been constantly growing in the economy. To sustain the growth rate for the next 20 years, India needs to increase its primary energy supply to 3–4 times.[11–15] By 2030, the power generation capacity must increase to about 8,00,000 W from the current levels of about 1,60,000 MW (Planning Commission Report, 2006). A look at the current energy landscape shows India's dependence on fossil fuels for its energy needs.[16–20]

EXPERIMENTAL

Materials

Zinc chloride, Polyvinyl alcohol (Mol. Wt. 1,25,000 g/mol), Glutaraldehyde and NaOH are purchased from s.d. Fine Chemicals, India. Double distilled water was used throughout the experiment. All the reagents were used without further purification.

Synthesis of Zinc Oxide Nanoparticles

Preparation ZnO nanoparticles were synthesized by direct precipitation method using zinc chloride and NaOH as precursors as reported in the literature.[21] In this work, the aqueous solution (0.2 M) of zinc chloride ($ZnCl_2.6H_2O$) and the solution (0.4 M) of NaOH were prepared with deionized water, respectively. The NaOH solution was slowly added into zinc chloride solution at room temperature under vigorous stirring, which resulted in the formation of a white suspension. The white product was centrifuged at 3000 rpm for 30 min and washed three times with distilled water, and washed with absolute alcohol at last. The obtained product was calcined at 500 °C in air atmosphere for 3 hr to obtain fine ZnO powder.

Preparation of Nanocomposite Membranes

Poly vinyl alcohol (6 g) taken in 80 mL of water was stirred constantly until the solution became transparent slurry. The synthesized ZnO nanoparticles in the gravimetric ratio of 2.5, 5, and 10 wt. % with respect to weight of PVA were dispersed in 10 mL of water separately and sonicated for 120 min and added to the above prepared PVA solution. The whole mixture was stirred for about 24 h to obtain a homogeneous solution, which was poured on to a clean and dry glass plate with the help of doctor's knife to form membranes of uniform thickness. The caste membranes were kept at ambient temperature for drying; the dried membranes were peeled off from the glass plate. The fabricated nanocomposite membranes were designated as M-1, M-2 and M-3 that contained 2.5, 5, and 10 wt. % of ZnO respectively.

Membrane characterization

Fourier Transmission Infrared (FTIR) spectral studies

FTIR spectra were taken for PVA before and after loading of NP's. Samples were scanned to confirm the crosslinking of PVA with ZnO in PVA matrix using Nicolet-740 and Perkin-Elmer-283B FTIR spectrophotometers. Membrane samples were ground well with KBr to make pellets under a hydraulic pressure of 400–450 kg/cm^2.

Scanning Electron Microscopic (SEM) Studies

SEM photograph of the ZnO loaded PVA membrane crosslinked with GA was taken. Membrane was sputtered with gold to make it conducting and placed on a copper stub. Scanning was done using high resolution (Mag. 300X 5 kV) using JOEL MODEL JSM 840A, scanning electron microscope (SEM),

X-ray diffraction studies

A Siemens D 5000 powder X-ray diffractometer was used to study the solid-state morphology of ZnO. X-rays of 1.5406 Å wavelength was generated by Cu Kα source. X-ray diffractograms of the ZnO nanoparticles. The angle of diffraction, 2θ was varied from 0° to 65° to identify any changes in the crystal structure and intermolecular distances between the inter-segmental chains. ZnO exhibits a typical peak at $2\theta = 7°$, which corresponds to (1 0 1) and (2 0 0) mixed planes. Diffraction patterns of the particles show that intensity of the peak decreased around $2\theta = 20°$.

Optical Microscopy Study

Olympus BX Series Upright Metallurgical Microscopes with model number BX53M was employed in the optical microscopy study. The prepared nanocomposite membranes samples as 2X2 cm square pieces were cut and mounted in the microscope. The size relative to the image projected onto the surface of the imaging array by the microscope optical system. When attempting to match microscope optical resolution to a specific digital camera, for determining the minimum pixel density necessary to adequately capture all of the optical data from the microscope.

Mechanical Properties

The purpose of studying tensile strength is that to study the mechanical property of the prepared membranes. To check under the H_2 and O_2 atmosphere in the fuel cell, at what extend the prepared membrane is durable. Mechanical properties of the plain PVA and ZnO loaded PVA membrane

strips were evaluated using the universal testing machine (UTM) (Hounsfield, UK), model H 25 KS, with an operating head load of 5 kN, following the procedure outlined in ASTM D-638 test method. Cross sectional area of the sample of known width and thickness was calculated. Membrane strips were placed between grips of the testing machine. The grip length was 5 cm; while the speed of testing was set at 5 mm/min. Tensile strength was calculated using the equation (1):

$$TensileStrength = \frac{Max\ Load}{Cross\ Sectional\ Area} \quad (1)$$

Fuel cell Measurements

The Na-Tungstate loaded PVA-g-AAm were sandiwiched in between Toray carbon papers chrged with a Pt as catalyst with loading of 0.5 mgPt cm^{-2} ((10 wt. % Pt)/Vulcan ®), ElectroChem SA) at anode and cathode ends. The effective membrane area is 4.8 cm^2. PEMFC was operated at 50°C with the flow rate of 150 mL min^{-1} of hydrogen with pressure 1 kg/cm^2 and 300 mL min^{-1} of air with pressure 1 kg cm^{-2}. The relative humidity maintained during the experiments was 75%, 90% and 100%. The proton conductivity (s) was obtained using the following formula (2),

$$\sigma = \frac{l}{R \times A} \quad (2)$$

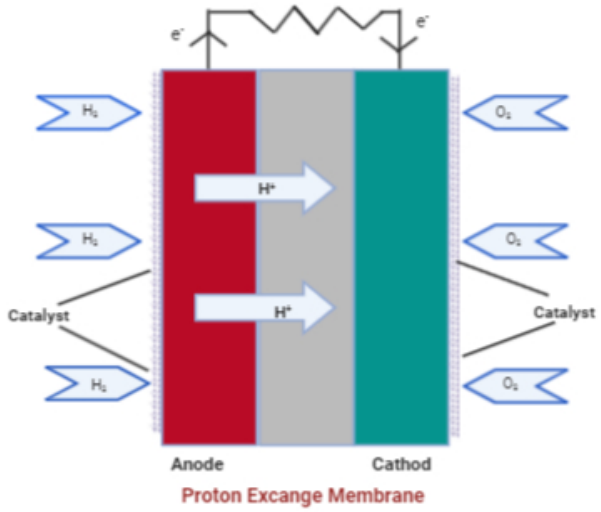

Fig. 1 – Fuel cell assembly illustration.

Where's' is the proton conductivity measured in terms of S cm^{-1}, 'l' is the membrane thickness (distance between electrodes) measured in cm and 'A' is the effective membrane area or the surface area required for proton transport across the membrane (or electrode area) and is measured in terms of cm^2 and 'R' is the resistance of the membrane (W). The illustration of fuel cell assembly was shown in Figure 1.

RESULTS AND DISCUSSION

Fourier transform infrared spectroscopy Study

FTIR (Fourier transform infrared spectroscopy) spectra of poly vinylalcohol, Blend with ZnO hybrid membranes were taken in the range between 4000 and 400 cm^{-1} to confirm the crosslinking of PVA with using Shimadzu IR Affinity-I FTIR spectrometer. Membrane samples were grounded well with KBr and pellets were formed by pressing under the hydraulic pressure of 400–450 kg/cm^2. FTIR spectral curves are displayed. All membranes used here are crosslinked with glutaraldehyde. Abroad peak at 3200 cm^{-1} for plain PVA represents OH stretching vibrations of the OH group. In the region of 1000–1100 cm^{-1}, multiple bands have appeared for plain alginate due to C-O stretching vibrations. In case of hybrid matrix membrane, the intensity of this peak was increased, indicating the formation of C-O-C bonds between linear alkyl chains (-CH_2-CH). However, -C-O- stretching is also observed in the same region as that of C-O stretching. The FTIR tracings are shown in Fig. 2.

X-ray diffraction studies

A Siemens D 5000 powder X-ray diffractometer was used to study the solid-state morphology ZnO nanoparticles. The XRD pattern of ZnO Nanoparticles was displayed in figure 3. X-rays of 1.5406 Å wavelength was generated by Cu Kα source. X-ray diffractograms of the ZnO nanoparticles. The angle of diffraction, 2θ was varied from 0° to 65° to identify any changes in the crystal structure and intermolecular distances between the inter-segmental chains. ZnO exhibits a typical peak at 2θ =32–37°, which corresponds to (1 0 0) and (1 0 1) mixed planes. Diffraction patterns of the particles show that intensity of the peak decreased around 2θ =47°.

Optical Microscopy Study

The optical microscopic study with the magnification X60 shown in the Figure 4. According to the study one can observe the surface of the all membranes are found to be rough in nature. Which are the key points to start diffusion of the molecules and facilitate to attract the like molecules.

Scanning Electron Microscopy (SEM) Studies

Surface SEM micrographs of, blend PVA, ZnO composite membranes were obtained under high resolution (Mag. 300X 5 kV) using JOEL MODEL

JSM 840A, scanning electron microscope (SEM), equipped with Phoenix energy dispersive analysis of x-rays (EDAX). SEM micrographs were taken. The SEM images were displayed in Figure 5. Micrographs of PVA-ZnO nanocomposite membranes were obtained under similar resolutions (Mag. 2KX) using Leica Stereoscan-440 SEM equipped with Phoenix energy dispersive analysis of x-rays (EDAX). Since all these films were nonconductive, gold coating (15 nm thicknesses) was done on samples. The Figure 5 (a) represents the plain PVA membrane and found uniform and the Figure 5 (b) PVA-ZnO (7.5 wt. %) membrane showing the uniform distribution of ZnO across the membrane matrix.

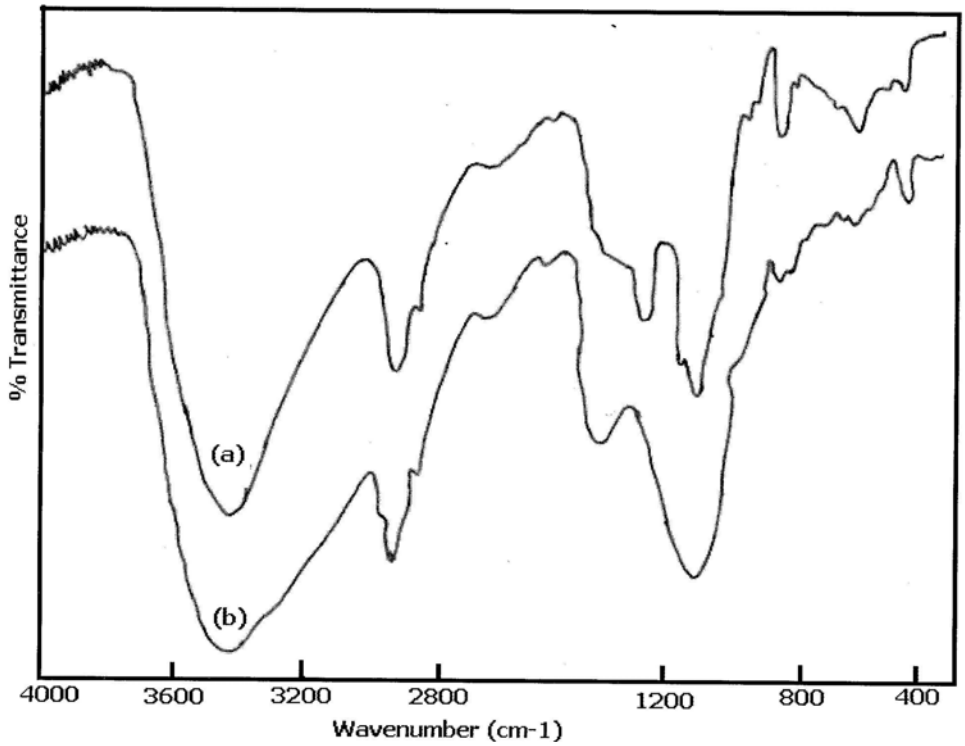

Fig. 2 – FTIR tracings of (a) Plain and (b) PVA-ZnO membranes.

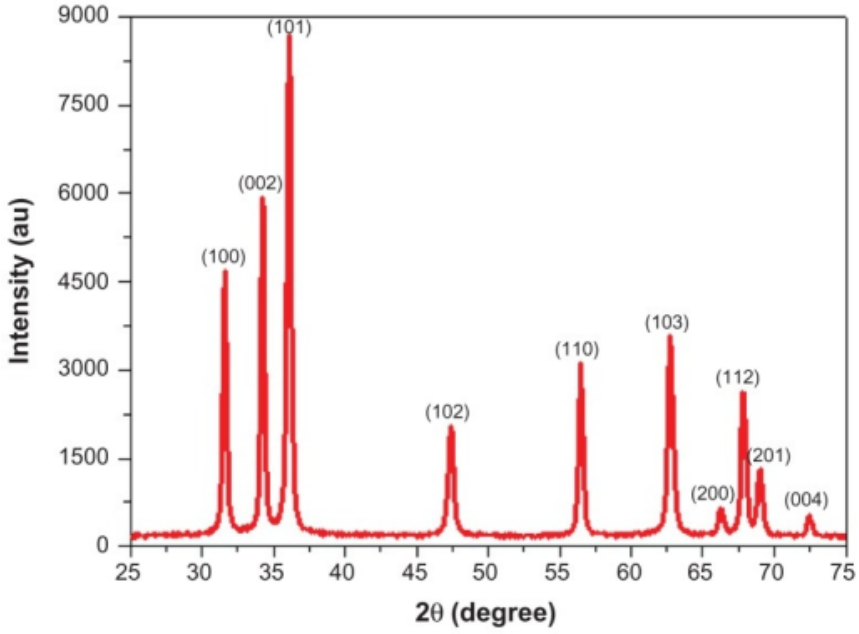

Fig. 3 – X-RD patterns of ZnO Nanoparticles.

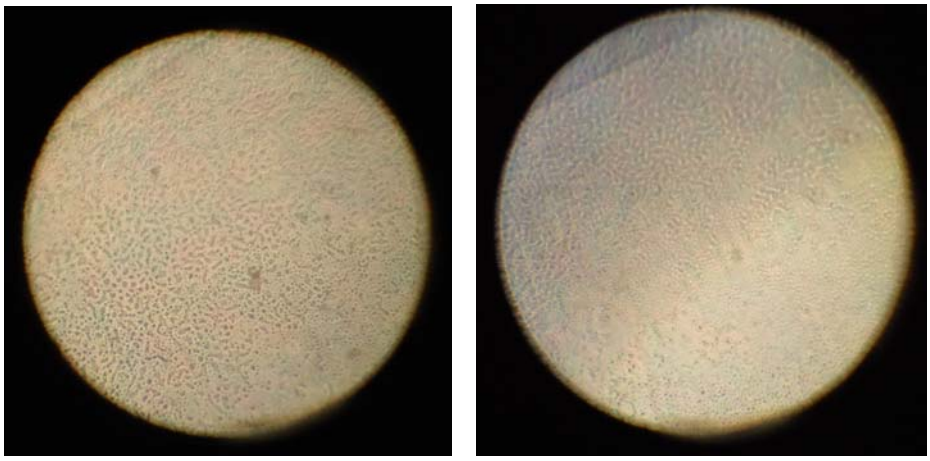

Fig. 4 – Optical microscopy of (a) plain PVA and (b) PVA loaded with ZnO (2.5 wt. %).

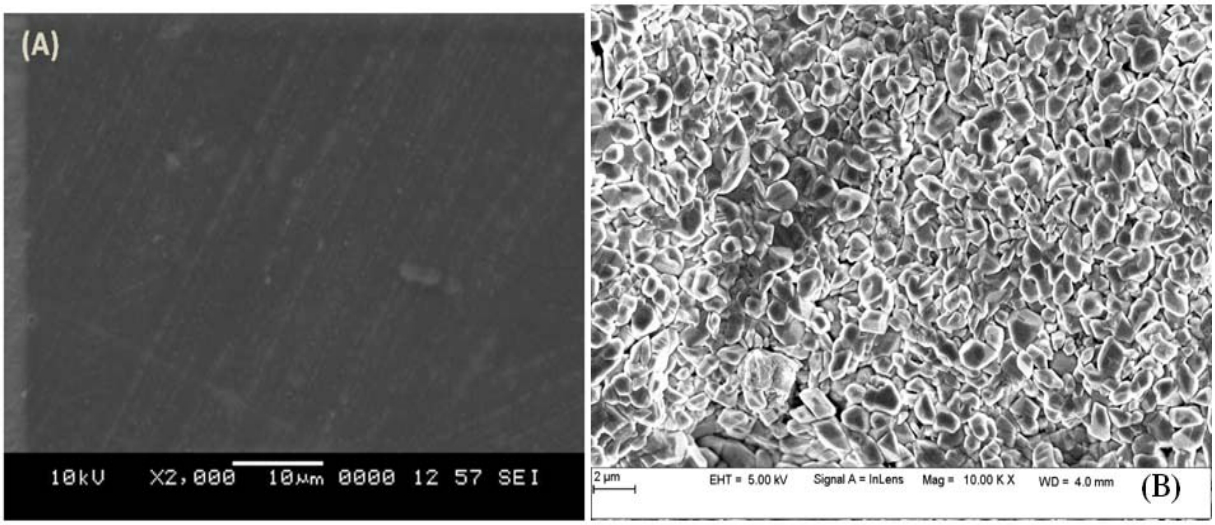

Fig. 5 – SEM images of (a) Plain PVA, (b) PVA-ZnO-7.5% membranes.

Mechanical Properties

Tensile strength data of plain PVA, M-1, M-2 and M-3 composite membranes were are presented in Table I. Among the four membranes tested PVA-ZnO-10 % exhibited highest tensile strength of **10.30** MPa. Consequently, tensile strength of PVA-ZnO-5 % was smaller than PVA-ZnO-10 % membrane, but that of plain PVA showed the least tensile strength of 3.83 MPa. These data suggest that after addition of ZnO nanoparticles to PVA, the mechanical strengths of the composite PVA membranes were improved due to crosslinking between PVA chains. The tensile strengths of the membranes followed the trend: PVA-ZnO-10 % > PVA-ZnO-5 % > PVA-ZnO-2.5 % > plain PVA. Increased mechanical strength of the ZnO-reinforced PVA is the result of favorable physicochemical interactions between ZnO nanoparticles and the PVA matrix.

Fuel cell tests

Synthesized ZnO loaded PVA membranes were tested for fuel cell using Hydrogen and Oxygen. The proton conductivity plots have been obtained shown in Figure 6. Results are shown for all prepared membranes i.e. M-1, M-2 and M-3. The obtained data shown that the modified membranes showed better performance as compared to its plain membrane. The plain membrane showed 3.492 x 10^{-2} S $cm^{-1}$for 75 % RH to 3.942 x 10^{-2} S cm^{-1}. Whereas 5 wt. % NA-Tungstate loaded Membranes showed 6.315 to 13.333 x 10^{-2} S cm^{-1} for 75% to 100% RH. The results showed that the increased proton conductivity as increase in humidity level and % loading of Na-Tungstate. The enhanced proton conductivity is achieved because of incorporation of small amount of Na-Tungstate in the base polymer moiety.

Table 1

Mechanical Strength of the various prepared membranes

Membrane Type	Tensile Strength MPa
Plain PVA	4.93
M-1	5.52
M-2	8.99
M-3	11.44

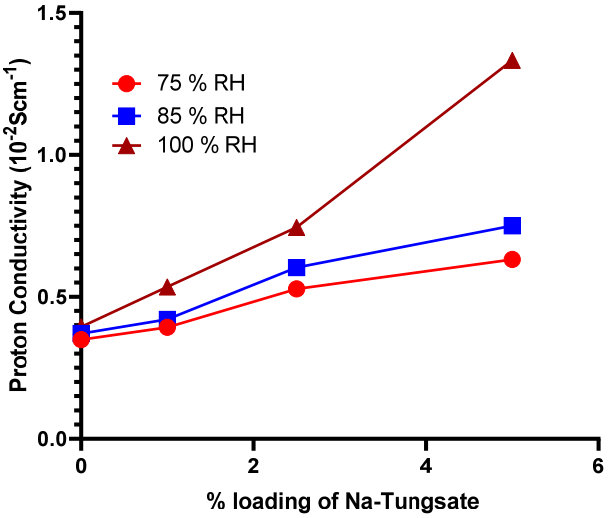

Fig. 6 – Proton conductivity curves for the different Na-Tungstate loaded membranes.

Scope of the Future Work

A fuel cell is one of the recently identified electrical energy resources which undergoes certain chemical reactions to produce electrical power using hydrogen as fuel and oxygen as an oxidizing agent. The classification of fuel cells based on the types of fuel used is explained. This research mainly focuses on comparative performance analysis of emulating behaviour of well-known fuel cells systems such as Proton Exchange Membrane Fuel Cell and Solid Oxide Fuel Cell for grid applications and standalone systems. Both PEMFC and SOFC have valuable attractive properties like high efficiency and hence the impacts of these fuel cells on the distribution network are determined and compared by using computational simulations.

CONCLUSIONS

To improve membrane performance, one can generally follow two distinct strategies, i.e., either to synthesize new polymers with specific chemical architectures or to modify the existing polymers by incorporating suitable fillers. This paper reports results obtained according to the latter route. It is realized from the literature that fillers like molecular organic framework (MOF) can improve separation properties of membranes, provided that appropriate zeolite and polymer combinations are chosen. The ZnO types of MOF filled PVA hybrid nanocomposite membranes of this study had not been previously reported in the literature. The mixed matrix nanocomposite membranes studied here were effective in fuel cell applications 2.5 to 10 wt. % with respect to the polymer matrix. The addition of even a small amount of ZnO nanoparticles into PVA membranes has improved both flux and selectivity to water over that of the plain PVA membrane. The prepared mixed matrix membranes were shown moderate response to the measured fuel cell.

Acknowledgements. Authors are greatful to the B. V. V. Sangha, Bagalkot for providing research facilities and Sri. Ashok M. Sajjan (Bewoor), Chairman, College Governing Council, Basaveshwar Science College, Bagalkot for his continuous support towards our research work.

REFERENCES

1. M. C. M. Alves, J. P. Dodelet, D. Guay, M. Ladouceur and G. Tourillon, *J. Phys. Chem.*, **1992**, *96*, 10898–10905.
2. (a) G. Andreadis, S. Song and P. Tsiakaras, *J. Power Sources*, **2006**, *193*, 555–561; (b) S. Ashley, *Sci. Am.*, **2005**, *292*, 62–69.

3. M. H. Atwan, D. O. Northwood and E. L. Gyenge, *Int. J. Hydrogen Energy*, **2005**, *30*, 1323–1331.
4. L. Barbora, S. Acharya, R. Singh, K. Scott and A. Verma, J. Membr. Sci., **2009**, *326*, 721–726.
5. S. Basu, "Recent trends in fuel cell science and technology", Springer, New York, 2007.
6. S. Basu, A. Agarwal, H. Pramanik, *Electrochem. Commun.*, **2008,** *10*, 1254–1257.
7. D. Basu and S. Basu, *Electrochim. Acta*, **2010**, *55*, 5575–5579.
8. J. Batista, A. Pintar, J. P. Gomilsek, A. Kodre and F. Bornette, *Electrochim. Acta*, **2001**, *56*, 6106–6113.
9. (a) J. Batista, A. Pintar, J. P. Gomilsek, A. Kodre, F. Bornette, *Appl. Catal. A: Gen*, **2021**, *217* 55–68; (b) L. Cao, G. Sun, H. Li and Q. Xin, *Electrochem. Commun.*, **2007**, *9*, 2541–2546.
10. F. Colamati, E. Antolini and E. R. Gonzalez, *J. Power Sources*, **2006**, *157*, 98–103.
11. Y. Daiko, L. C. Klein, T. Kasuga and M. Nogami, *J. Membr. Sci.*, **2006**, *281*, 619–625.
12. R. F. B. De Souza, G. S. Buzzo, J. C. M. Silva, E. V. Spinacé, A. O. Neto, M. H. M. T. Assumpção, *Electrocatalysis*, **2014**, *5*, 213–219.
13. G. Faubert, G. Lalande, R. Côté, D. Guay, J. P. Dodelet, L. T. Weng, P. Bertrand and G. Dénès, *Int. J. Electrochem. Sci.*, **1996**, *5*, 895–902.
14. G. Faubert, G. Lalande, R. Cote, D. Guay, J. P. Dodelet, L. T. Weng, B. Patrick, G. Denes, *Electrochim. Acta,* **1996**, *41*, 1689–1701.
15. R. Ganesan and J. S. Lee, *Angew. Chem. Int. Ed.*, **2005**, *44,* 6557–6560.
16. Y. Gao, G. Q. Sun, S. L. Wang and S. Zhu, *Energy*, **2010**, *35,* 1455–1459.
17. M. B. Patil, *Mater. Sci. for Energy Techn.*, **2020**, *3,* 846–852.
18. N. H. Behling, *J. Electrochem. Soc.*, **2002**, *149*, A256–A326.
19. J. J. Junpei Miyake, Y. Ogawa, T. Tanaka, J. Ahn, K. Oka Oyaizu and K. Miyatake, *Commun. Chem.*, **2020**, *3*, 1–7.
20. Z. Wang, H. Li, F. Tang, J. Ma and X. Zhou, *Nanoscale Research Lett.*, **2018**, *13*, 1–9.